



Estimation of Heat Production Rate using Thermal Data During Exercise in Indoor Environments: A Study of Heat Storage Rate in Male Athletes

Gorkem Aybars Balci¹ · Ali Berkay Avci² · Muzaffer Colakoglu¹ · Tahsin Basaran²

Received: 27 June 2023 / Revised: 29 December 2023 / Accepted: 3 March 2024 / Published online: 15 March 2024
© The Author(s) under exclusive licence to International Society of Biometeorology 2024

Abstract

The increasing preference for indoor exercise spaces highlights the relationship between indoor thermal environments and physiological responses, particularly concerning thermal comfort during physical activity. Determining the metabolic heat production rate during exercise is essential for optimizing the thermal comfort, well-being, and performance of individuals engaged in physical activities. This value can be determined during the activity using several methods, including direct calorimetry measurement, indirect calorimetry that uses analysis of respiratory gases, or approximations using collected data such as speed, body mass, and heart rate. The study aimed to calculate the metabolic heat production rate by infrared thermal evaluation (ITE) based on the body's thermal balance approach and compare it with the values determined by indirect calorimetry (IC). Fourteen participants volunteered for the study, using a cycling ergometer in a controlled climatic chamber. After the familiarization sessions, maximal O₂ intake levels (VO_{2max}) were determined through maximal graded exercise tests. Subsequently, constant work rate exercise tests were performed at 60% of VO_{2max} for 20 min. The metabolic heat production rates were calculated by IC and ITE for each athlete individually. Respiratory gases were used to determine IC, while body skin and core temperatures, along with physical environmental data, were applied to calculate ITE using the human body thermal balance approximation of ASHRAE. According to the results, heat storage rates were misleading among the body's heat transfer modes, particularly during the first 8 min of the exercise. ITE showed a moderate level of correlation with IC (r: 0.03–0.86) with a higher level of dispersion relative to the mean (CV%: 12–84%). Therefore, a new equation (ITE_{new}) for the heat storage rates was proposed using the experimental data from this study. The results showed that ITE_{new} provided more precise estimations for the entire exercise period ($p > 0.05$). Correlations between ITE_{new} and IC values were consistently strong throughout the exercise period (r: 0.62–0.85). It can be suggested that ITE_{new} values can predict IC during the constant work rate steady-state exercise.

Keywords Body heat storage · Body thermal balance · Exercise · Infrared thermography · Thermoregulation

Introduction

In recent years, there has been a notable shift in the trend toward indoor exercise spaces, with a growing number of individuals preferring indoor environments for their physical activities (Lanza et al. 2022; Dahlan et al. 2023). This demand for indoor spaces highlights the intricate relationship between indoor thermal environments and human physiology. Metabolic energy rate (M) is the rate at which the body produces energy through metabolic processes, including the conversion of energy derived from food consumption (Wasserfurth et al. 2020). This energy is utilized to sustain homeostasis and support physical activity. During

✉ Ali Berkay Avci
aliavci@iyte.edu.tr
Gorkem Aybars Balci
gorkem.aybars.balci@ege.edu.tr
Muzaffer Colakoglu
muzaffer.colakoglu@ege.edu.tr
Tahsin Basaran
tahsinbasaran@iyte.edu.tr

¹ Department of Coaching Education, Ege University, Faculty of Sport Sciences, Izmir, Turkey

² Department of Architecture, Izmir Institute of Technology, Izmir, Turkey

physical exercise, a portion of this metabolic energy rate is converted into mechanical work rate (W), representing the measurable physical output by the muscles (Parsons 2014). The remaining energy is transformed into heat, known as the net metabolic heat production rate ($M-W$), which must be efficiently released to the environment (ASHRAE 2009). Indoor thermal environmental factors, including air temperature, radiant temperature, relative humidity, and air velocity, significantly influence the proper functioning of the human body's energy balance (Kang et al. 2022). Therefore, understanding the metabolic heat production rate during exercise in indoor environments is crucial for optimizing individuals' performance, thermal comfort, and well-being in indoor exercise routines.

The amount of energy consumed during physical activity can be measured by calculating produced heat and mechanical energy or by analyzing respiratory gases. Responses such as energy expenditure corresponding to frequently varying effort intensities during physical activity, lactate production in the blood, heart rate (HR), oxygen consumption (VO_2), carbon dioxide production (VCO_2), and respiratory exchange ratio (RER) help analyze the performance of the athletes (Whipp et al. 1982). About 15–25% of the energy during exercise is spent on mechanical work, while the remaining portion is transferred to the immediate surroundings and stored inside the body as thermal energy (Flouris and Schlader 2015). Therefore, a significant part of energy production corresponds to thermal energy.

Many studies have been carried out to determine heat and mass interaction between the human body and the environment (Havenith 2001; Takada et al. 2009; Qingqing and Jianhua 2020; Qi et al. 2022; Greenfield et al. 2023; Lin et al. 2023). In these studies, it was stated that thermal sensitivity levels differ in various parts of the body. For this reason, examining the body by dividing it into regions is recommended to consider the thermal sensitivity changes (Tanabe et al. 1995). Most studies on the numerical determination of heat and mass interaction between the human body and the environment adopted the thermal balance approach that accepts the human body as a two-layered cylinder, introduced by Gagge et al. (Gagge, A. P., Fobelets, A. P. and Berglund 1986). The outer layer of this cylinder represents the skin, and the inner one represents the body's core. In this approach, the body's metabolic heat production rate equals the heat transfer rate from the body to the environment and heat storage rate within the body. The energy transfer from the body to the environment includes evaporative, radiative, conductive, and convective heat losses from the skin and latent and sensible heat losses by respiration.

There are several studies on the calculation of heat production rate using the body's thermal balance approach during physical exercise (Bain et al. 2011; Vargas et al. 2019a;

Ravanelli et al. 2020). However, upon examining these studies, it becomes apparent that the required evaporative heat transfer rate (E_{req}) and required heat storage rate (S_{req}) were calculated using parameters obtained from indirect calorimetry. Determining heat transfer modes under exercise conditions without employing indirect calorimetry is yet to be the focus of any study within the authors' knowledge. However, determining E_{req} and S_{req} might be possible if the storage rates in the skin (S_{sk}) and core (S_{cr}) are carefully evaluated, as they are significant energy exchange modes during physical exercise in the body's energy balance equation (Kenny et al. 2008). Calculating these stored energy modes based on thermal data can be accomplished using changes in skin and core temperatures per unit of time (ASHRAE 2009). Nevertheless, it is well-known that depending on the recording method and exercise intensity, skin and core temperature changes per unit of time vary considerably (Torii et al. 1992; Zontak et al. 1998; Merla et al. 2010; Tanda 2018; Kasprzyk et al. 2019). Therefore, it is crucial to accurately measure skin and core temperatures using appropriate methods to calculate S_{sk} and S_{cr} during exercise.

The study aims to calculate the metabolic heat production rate during exercise with the thermal balance approach of the human body by using the values of skin and core temperatures and the necessary environmental data. This study hypothesizes that the metabolic heat production rates calculated by infrared thermal evaluation (ITE) can be used at steady-state exercise.

Materials and Methods

Participants

A total of 14 male athletes who competed in cycling, triathlon, and track and field voluntarily participated in the study, which was approved by the Ege University Ethics Committee. All participants were healthy and physically active, engaging in at least three endurance training sessions per week (age: 23.8 ± 3.2 years; height: 1.79 ± 0.07 m; mass: 73.7 ± 7.6 kg; body mass index: 22.9 ± 1.9 $kg \cdot m^{-2}$; body fat percentage: $11.2\% \pm 2.6$; VO_{2max} : 50.4 ± 5.8 $mL \cdot min^{-1} \cdot kg^{-1}$). To capture infrared thermographic imaging across a wider body surface area, participants underwent the twenty-minute constant work rate exercise tests wearing only 100% cotton short pants and socks, along with sports shoes. The selection of cotton fabric was made due to its permeability to air and water vapor, along with its easy availability in the market. Based on these features of cotton as a natural material, it was selected to ensure participants' comfort sensation during exercise.



Fig. 1 Inside and outside views of the test chamber

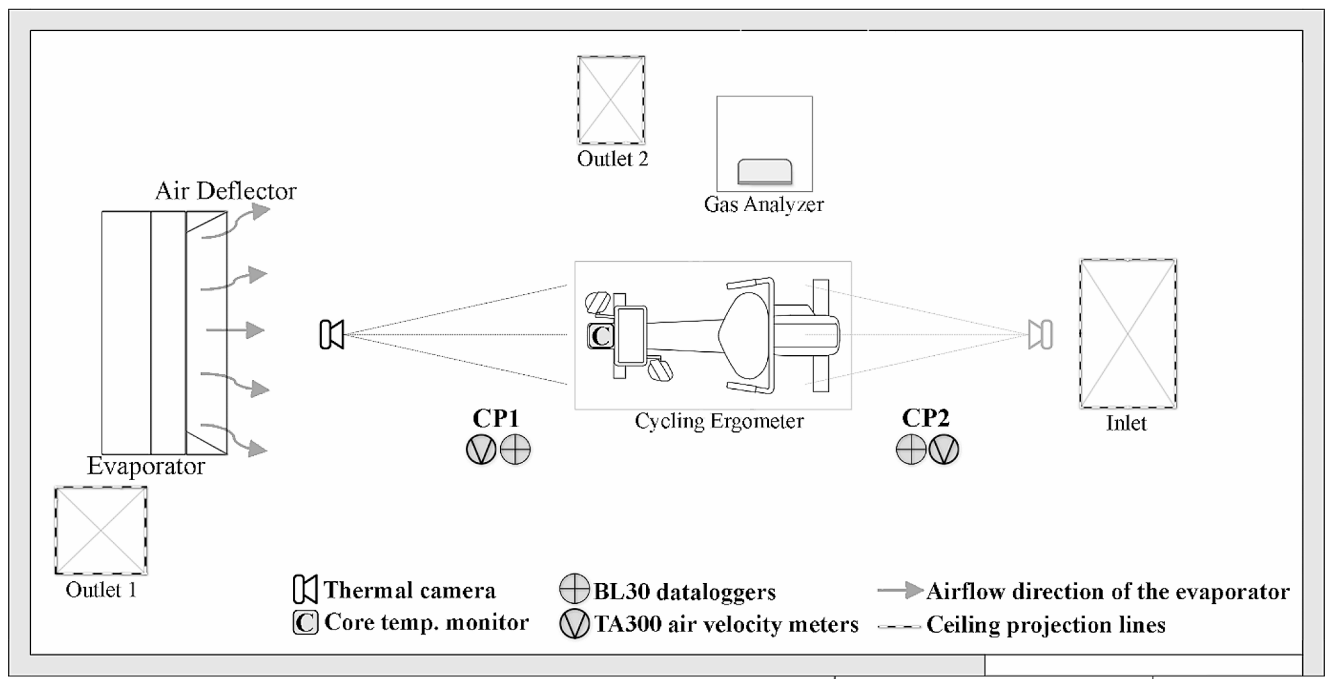


Fig. 2 Schematic plan of the experimental setup in the climatic chamber

Experimental Design

The study was conducted under normothermic and normoxic conditions in a climatic chamber with a continuous fresh air supply (Fig. 1), where the temperature and relative humidity were constantly monitored and adjusted (21 ± 0.2 °C, $51 \pm 1\%$ RH, $O_2 > 20.5\%$, $CO_2 \leq 450$ ppm). The chamber’s conditioning system maintained predetermined indoor thermal conditions through sensor-controlled automation, regulating temperature and relative humidity to ensure a stable environment during experiments. Additionally, fresh

air supply was monitored using CO_2 sensors. Forty minutes before the start of each exercise test, the conditioning system was activated to ensure the climatic test chamber reached the specified environmental conditions.

The climatic chamber measures 4 meters in width, 6 meters in length, and has a height of 3 meters. Within the test chamber depicted in Fig. 2, there are three ceiling vent holes: the “Inlet” is connected to a fan coil and a heat recovery unit, “Outlet 2” works with the heat recovery unit, and “Outlet 1” directs interior air to the fan coil unit before reaching the “Inlet” section. The fan coil unit is equipped

with two 3 kW electrical heaters and an integrated humidification system. On the other hand, the heat recovery unit transfers exhaust air energy to the supply air from “Outlet 2” before discharging it into the atmosphere. The internal evaporator unit of the cooling system removes excess heat when the indoor air temperature rises above the predetermined level with a ± 1 °C divergence. In order to ensure uniform air distribution and prevent direct exposure of the participant’s back to cooler air, an air deflector has been installed in front of the evaporator. A mechanical resistance bicycle ergometer (Monark 894 Ergomedic E; Sweden) located at the center of the chamber was used during the exercise tests, as shown in Fig. 2.

Firstly, the familiarization sessions lasting 20 min were conducted to help participants adapt to the experiments and to determine the initial work rates for the submaximal VO_2 tests. Subsequently, after a period of 24–48 h, submaximal VO_2 tests lasting 20 min were initiated to establish the initial work rate for the $\text{VO}_{2\text{max}}$ tests. Approximately 45–60 min later, $\text{VO}_{2\text{max}}$ tests, lasting 10–12 min, were conducted to determine the work rate for the submaximal constant work rate exercise. After another 24–48 h, twenty-minute submaximal constant work rate exercise tests were performed at 60% of $\text{VO}_{2\text{max}}$, constituting the main experimental session of the study. The details of the exercise test sessions are presented in the ‘Experimental Procedures’ section.

In order to achieve a thermally balanced condition for participants and mitigate the influence of their activities before the twenty-minute exercise test, they were given about 15 min in the climatic chamber, during which their core temperatures were monitored. Indoor air temperature (T_a), relative humidity (RH), and air velocity (V_a) measurements from two control points (CP1 and CP2 in Fig. 2), located at a distance of one meter from the front and back of the participants, were taken during twenty-minute exercise period to be used in the metabolic heat production rate calculations. The details of the environmental and physiological measurements are provided in the ‘Experimental Procedures’ section. The schematic plan of the climatic chamber setup is illustrated in Fig. 2.

In this study, metabolic heat production rates (M-W) were calculated from the thermal responses of the human body and the environmental data. This calculation process was called infrared thermal evaluation (ITE). At the same time, indirect calorimetry (IC), which corresponded to M-W, was measured experimentally with the gas analyzer. The initial two-minute period of the measurements was excluded from the calculations because VO_2 responses were not stabilized. The details of the calculations of human body heat production rates are presented in the ‘Experimental Procedures’ section. The steps for calculating metabolic heat production rates followed in the study are shown in Fig. 3.

Experimental Procedures

Respiratory Gas and Metabolic Rate Analyses

During the measurements, a gas analyzer (Quark b², COSMED, Rome, Italy) was used to determine oxygen consumption (VO_2), carbon dioxide production (VCO_2), respiratory exchange ratio (RER), oxygen consumption rate (Q_{O_2}), breathing frequency (Bf) and respiratory anaerobic threshold (AnT). Heart rate (HR) was recorded by an integrated part of the same equipment, and external heart rate was also monitored (Polar RS400; Polar Electro Oy, Kempele, Finland). The device was calibrated following the manufacturer’s instructions. The body surface areas of the participants were calculated using the DuBois formula (Du Bois and Du Bois 1989), and body fat percentages were determined using Jackson and Pollock’s seven-site equation (Jackson and Pollock 1978). To calculate the net metabolic heat production rates (M-W), mechanical work rate (W) values were subtracted from the metabolic rates (M). The necessary mechanical work rate of the participants was determined and monitored through the mechanical resistance bicycle ergometer (Monark 894 Ergomedic E; Sweden).

Metabolic Heat Production Rate Calculations by Indirect Calorimetry

Metabolic heat production rates by indirect calorimetry were calculated using E.1, E.2, and E.3 (Nishi 1981).

$$M = [21 \times (0.23 \times \text{RER} + 0.77) \times Q_{O_2}] / A_D \quad [\text{E.1}]$$

$$A_D = 0.202 \times \text{mass}^{0.425} \times \text{height}^{0.725} \quad [\text{E.2}]$$

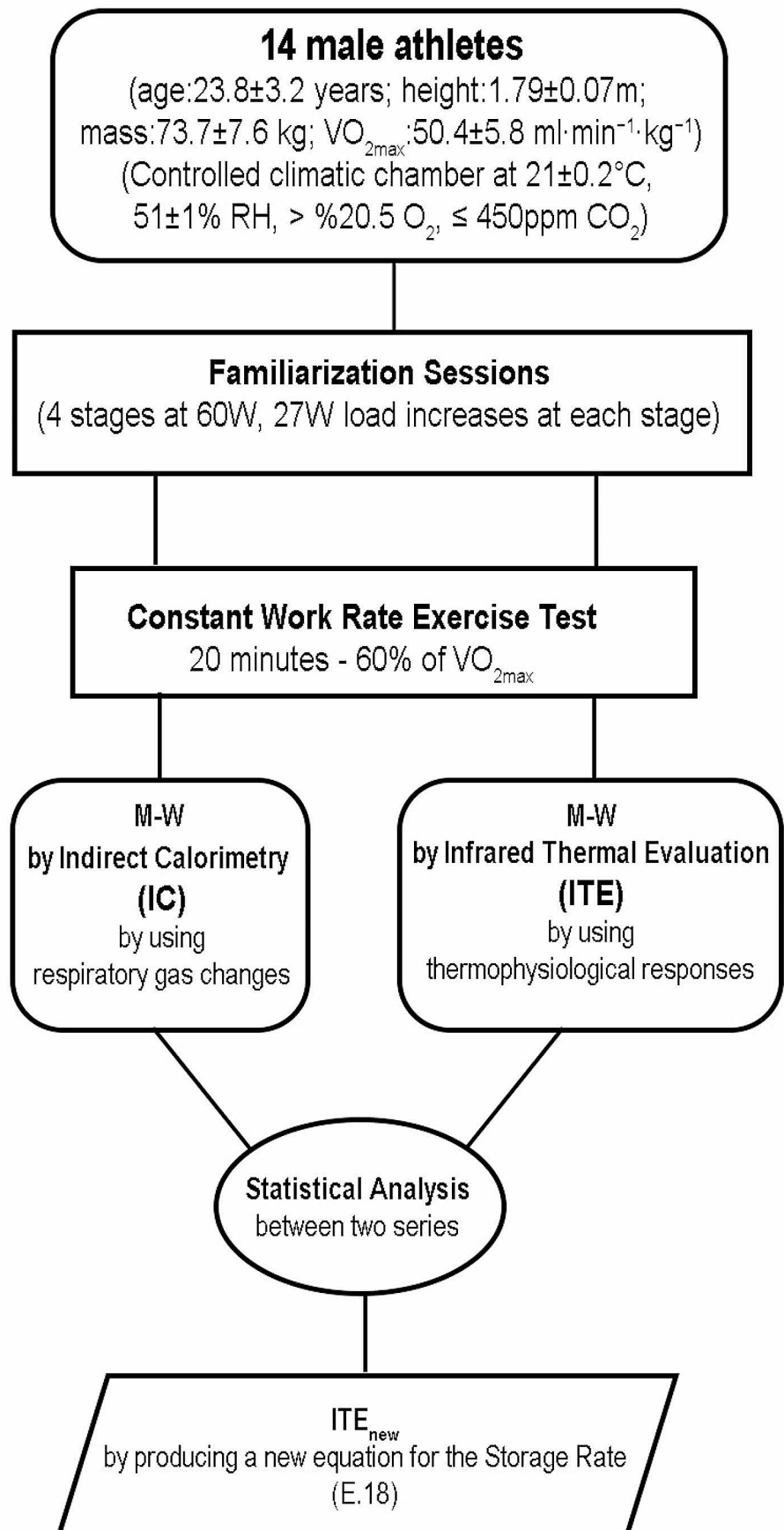
$$\text{IC} = M - W \quad [\text{E.3}]$$

M: Metabolic rate ($\text{W}\cdot\text{m}^{-2}$); RER: Respiratory exchange ratio; Q_{O_2} : Oxygen consumption rate ($\text{mL}\cdot\text{s}^{-1}$); A_D : DuBois body surface area (m^2); IC: Metabolic heat production by indirect calorimetry ($\text{W}\cdot\text{m}^{-2}$); M-W: Metabolic heat production rate ($\text{W}\cdot\text{m}^{-2}$)

Core and Skin Surface Temperature Measurement

Skin temperatures of the athletes were measured using an infrared camera with a resolution of 160×120 pixels and thermal sensitivity below 0.08 °C (Testo 875-1 ThermoCAM, Germany). Participants underwent a fifteen-minute resting period in a seated position inside the climatic chamber to ensure stabilized thermal balance before the exercise tests (Marins et al. 2014). The skin temperature measurements were taken 1.5 m in front of and behind the participants’ bodies at a 90° angle, as shown in Fig. 2. In thermal camera measurements, the emissivity of the body surface was considered as 0.95 (Çengel 2003), and temperature

Fig. 3 Flow chart of the study



analysis was performed using the computer software. During the tests, measurements by the infrared camera were taken every two minutes (Fig. 4). The skin temperature measurements followed the method used in the study by Balci et al. (2016), where an average of two body regions was included. Average temperatures from the selected body regions were recorded by drawing ovals around the chest (T_{chest}) and back (T_{back}). Subsequently, mean skin temperature values were determined using the equation " $T_{\text{sk}} = (T_{\text{chest}} + T_{\text{back}}) / 2$ " (Balci et al. 2016; Zora et al. 2017; Avci et al. 2024).

Measurements of core temperature were done by swallowable temperature sensors that can continuously transmit data telemetrically to their monitor, to which these sensors transfer the responses (VitalSense; Philips Respironics, the Netherlands), as shown in Fig. 2. The subjects were ensured to take temperature pills four hours before the tests. During the twenty-minute constant work rate exercise tests, the core temperature monitor was positioned under the saddle of the stationary bicycle, closer to the participants, where it could read data from the sensors.

Indoor Environmental Measurements

Indoor air temperature (T_a), relative humidity (RH), and air velocity (V_a) measurements were conducted from two control points (CP1 and CP2 in Fig. 2) to be used in the calculations of metabolic heat production rate. These control points were positioned one meter away from the front and back of the participants, ensuring that the measurements

represented the values affecting the participants during the twenty-minute exercise period. Air velocity measurements were obtained using two Trotec TA300 air velocity meters with an accuracy of $\pm 5\%$ of the measured value + 1 digit, as denoted in Fig. 2 of Sect. 2.2. Air temperature and relative humidity measurements were recorded by two Trotec BL30 dataloggers ($\pm 1\text{ }^\circ\text{C}$, $\pm 3\%$), as given in Fig. 2 of Sect. 2.2. All data were recorded at five-second intervals. The CO_2 levels inside the room were recorded by the sensors of the automation system, and this data were monitored using the external control panel of the climatic chamber. The averages of the environmental measurements from the two control points were used in the calculations of metabolic heat production rate, computed as two-minute averages.

Familiarization Sessions

Participants were subjected to familiarization sessions to obtain their anthropometric measurements and adapt to the environment (bicycle ergometer, air conditioning room, and study group). The main objective of these familiarization sessions was to determine the participants' initial work rate for the submaximal VO_2 tests. During these sessions, the participants engaged in exercises in four stages, each lasting five minutes (20 min in total). The exercise started with a workload of 60 W, and the workload was increased by 27 W at each stage (Balci et al. 2016; Avci et al. 2024). The HR and respiratory gas responses were recorded during exercise.

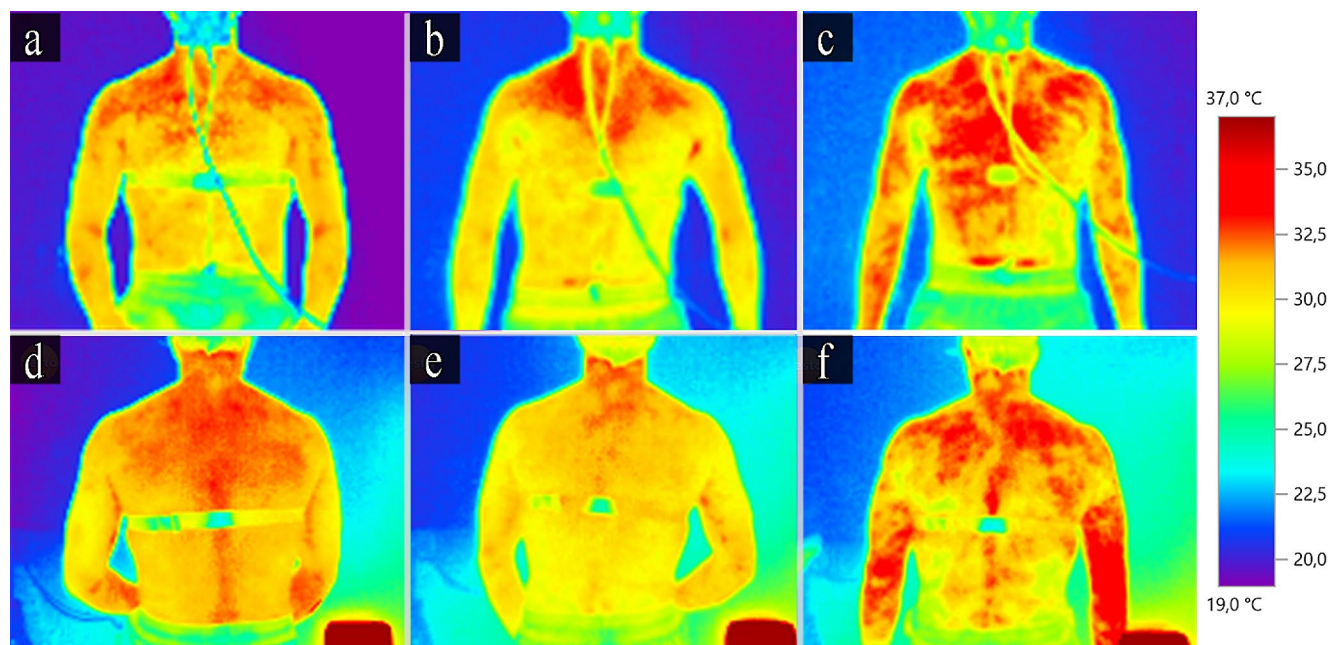


Fig. 4 Infrared thermal camera measurements at (a) 4th minute, front; (b) 8th minute, front; (c) 20th minute, front; (d) 4th minute, back; (e) 8th minute, back; (f) 20th minute, back

VO₂ Submaximal Test

VO₂ submaximal tests were applied to obtain the exercise work rate, indicating the approximate AnT value of each participant. A four-step submaximal test was initiated, considering the recorded data in the familiarization sessions. Each stage lasted five minutes with a load corresponding to 50–60% of HR_{max} (20 min in total). After continuing with 27 W increments, the test was terminated when the participants reached 70–85% of the maximal heart rate (Maximal HR: 220-age). AnT was calculated from the v-slope method (Schneider et al. 1993).

VO_{2max} test

The graded maximal exercise tests were initiated following a 45–60-minute resting period performed after the submaximal tests. The initial work rate was set based on the AnT. Participants were instructed to maintain a fixed cadence of 90 rpm throughout the test. The test continued until the participants reached volitional exhaustion, following a protocol with load increases of 27 W every two minutes (lasting 10–12 min in total). VO_{2max} was recorded as the highest VO₂ value during the thirty-second period.

Submaximal Constant Work Rate Exercise

The constant work rate submaximal exercise was performed at a constant workload corresponding to 60% of VO_{2max} (below the AnT for each participant) at 90 rpm for 20 min after 24–48 h of the graded maximal exercise test. Variables, including T_a, RH, V_a, VO₂, VCO₂, and HR, were measured instantly and averaged at two-minute intervals. T_{sk} and T_{cr} responses were recorded every two minutes. The data calculated in this exercise test were used in the calculations of metabolic heat production rate.

Metabolic Heat Production Rate by Infrared Thermal Evaluation

The net metabolic heat production rate values, determined by the human body thermal balance approach, were calculated as described in E.4.

$$ITE = (C + R + E_{sk}) + (C_{res} + E_{res}) + (S_{sk} + S_{cr}) \quad [E.4]$$

C + R: Heat loss rate through convection and radiation (W•m⁻²); E_{sk}: Evaporative heat loss rate through the skin (W•m⁻²); C_{res}: Respiratory sensible heat loss rate (W•m⁻²); E_{res}: Respiratory latent heat loss rate (W•m⁻²); S_{sk}: Heat storage rate in the skin compartment (W•m⁻²); S_{cr}: Heat storage rate in the core compartment (W•m⁻²); ITE: Metabolic heat production rate by infrared thermal evaluation (W•m⁻²)

Respiratory Losses

The total heat and moisture transfer through respiration during the twenty-minute submaximal exercise tests were calculated by E.5. Pulmonary ventilation rates are recorded during the respiratory gas analysis.

$$(C_{res} + E_{res}) = \frac{\dot{m}_{res}(h_{ex}-h_a)}{A_D} \quad [E.5]$$

\dot{m}_{res} : Pulmonary ventilation rate (kg•s⁻¹); h_{ex}: Enthalpy of exhaled dry air (J•kg⁻¹); h_a: Enthalpy of ambient dry air (J•kg⁻¹)

Evaporative Heat Losses from the Skin

The evaporative heat loss from the skin depends on the water vapor pressure difference between the ambient air and the skin conditions individually (E.6, E.7, and E.8). The evaporative heat transfer coefficient was determined by the Lewis Ratio, which indicates the relationship with the convective heat transfer coefficient around the human body. The skin wettedness values were determined by following the procedures in ASHRAE (ASHRAE 2009).

$$E_{sk} = w \cdot h_e \cdot (p_{sk,s} - p_a) \quad [E.6]$$

$$LR = \frac{h_e}{h_c} \quad [E.7]$$

$$h_c = 8.3 \times V_a^{0.6} \quad [E.8]$$

h_e: Evaporative heat transfer coefficient (W•m⁻²•kPa⁻¹); P_{sk,s}: Water vapor pressure at skin, assumed to be at saturated vapor pressure (kPa); p_a: Water vapor pressure at ambient air (kPa); w: Skin wettedness; LR: Lewis ratio (16.5); h_c: Convective heat transfer coefficient (W•m⁻²•K⁻¹); V_a: Air velocity (m•s⁻¹)

Sensible Heat Losses from the Skin

Sensible heat losses from the skin occur through radiation and convection to the environment (ASHRAE 2009). In the study, these two heat loss modes were calculated by the following equations: E.9 and E.10. The required convective and radiative heat transfer coefficients were derived using E.11 and E.12.

$$C = h_{cc} (T_{sk} - T_a) \quad [E.9]$$

$$R = h_r (T_{sk} - T_r) \quad [E.10]$$

$$h_{cc} = h_c \left(\frac{p_t}{101.33} \right)^{0.55} \quad [E.11]$$

$$h_r = 4\epsilon \sigma \frac{A_r}{A_D} \left(273.2 + \frac{T_{sk} + T_r}{2} \right)^3 \quad [E.12]$$

h_{cc}: Corrected convective heat transfer coefficient (W•m⁻²•K⁻¹); T_a: Air temperature (°C); T_r: Radiant temperature (°C); h_r: Radiative heat transfer coefficient (W•m⁻²•K⁻¹); p_t: Local atmospheric pressure (kPa); ε: Emissivity of the skin; σ: Stefan-Boltzman constant (5.67 × 10⁻⁸ W•m⁻²•K⁻⁴); A_r: Radiative heat transfer area of the body (m²);

Rate of Heat Storage in the Body

The rate of heat storage in the body refers to an increase in the internal energy of the skin and core compartments. Each storage rate was calculated using equations E.13 and E.14. The required body mass skin fraction was determined using equations E.15 and E.16 every two minutes from each cycling individual (Gagge et al. 1972; ASHRAE 2009).

$$S_{cr} = \frac{(1-\alpha_{sk})m_{c,p,b}}{A_D} \times \frac{\Delta T_{cr}}{\Delta t} \quad [E.13]$$

$$S_{sk} = \frac{\alpha_{sk}m_{c,p,b}}{A_D} \times \frac{\Delta T_{sk}}{\Delta t} \quad [E.14]$$

$$\alpha_{sk} = 0.0418 + \frac{0.745}{Q_{bl}-0.585} \quad [E.15]$$

$$Q_{bl} = \frac{BFN+c_{dil} \times (T_{cr}-37)}{1+S_{tr} \times (34-T_{sk})} \quad [E.16]$$

α_{sk} : Fraction of body mass concentrated in skin compartment; m : Body mass (kg); $C_{p,b}$: Specific heat capacity of body ($3490 \text{ J}\cdot\text{kg}^{-1}\cdot\text{K}^{-1}$); T_{sk} : Temperature of skin compartment ($^{\circ}\text{C}$); T_{cr} : Temperature of core compartment ($^{\circ}\text{C}$); t : Time (s); Q_{bl} : Blood flow ($\text{L}\cdot\text{h}^{-1}\cdot\text{m}^{-2}$); BFN : Neutral skin blood flow ($\text{g}\cdot\text{m}^{-2}\cdot\text{s}^{-1}$); C_{dil} : Specific heat for skin blood flow ($\text{J}\cdot\text{kg}^{-1}\cdot\text{K}^{-1}$); S_{tr} : Skin blood flow constriction constant

Required Heat Storage Rate

Required heat storage rates (S_{req}) were acquired by subtracting the heat loss rates from the net heat production rate, calculated by indirect calorimetry, to compare the accuracy of the calculated total heat storage rate ($S_{cr}+S_{sk}$) as described in E.17.

$$S_{req} = (S_{sk} + S_{cr})_{req} = IC - C_{res} - E_{res} - E_{sk} - R - [E.17]$$

S_{req} : Required heat storage rate ($\text{W}\cdot\text{m}^{-2}$); IC : (M-W) Metabolic heat production rate by indirect calorimetry ($\text{W}\cdot\text{m}^{-2}$)

Statistical Analysis

Statistical analysis was performed using IBM SPSS Statistics (Version 21). After the Shapiro-Wilk normality test, the variance homogeneity of the participants was evaluated by the Levene test. The differences in the time-dependent changes of ITE and IC were evaluated by repeated-measures ANOVA. Bonferroni was used as a post-hoc. Pearson correlation analysis was employed to assess the relationship between the ITE and IC data of the participants. Furthermore, Pearson correlations of the heat transfer modes and ITE were presented to ensure that the most significant energy rate mode was the body heat storage rate during the twenty-minute exercise test. A linear regression model was created to demonstrate the effect of the temperature change per two minutes in the core and skin compartments (ΔT_{cr} and ΔT_{sk}) on S_{req} during the twenty-minute exercise period.

The developed equation was used to calculate S_{new} values and eventually to determine ITE_{new} values for each individual every two minutes. Effect size was analyzed based on Cohen's d . Data are presented as mean \pm standard deviation. For statistical analysis, the significance level was set at $p \leq 0.05$. To determine the statistical power of the linear regression model, G*Power 3.1.9.7 tool was utilized. This tool incorporated the sample size and R^2 value to assess the robustness of the estimation of statistical power.

Results

Skin and Core Temperature Responses

Before analyzing the metabolic heat production rates calculated by ITE and IC, it is significant to present the changes in the skin (ΔT_{sk}) and core (ΔT_{cr}) temperature responses monitored during the exercise tests. These body temperatures directly influence the heat storage rates within the body, indicating whether the body is storing heat or dissipating it to the environment. According to the thermal balance approach proposed by ASHRAE (ASHRAE 2009), changes in T_{cr} and T_{sk} are determinant factors used in the calculations of core and skin energy storage rates (E.13 and E.14). An increase in T_{cr} signifies an elevated core heat storage rate, while an augmentation in T_{sk} leads to higher levels of the skin's heat storage rate.

In this study, T_{sk} responses decreased during the first eight-minute period ($p \leq 0.05$), suggesting heat dissipation from the skin compartment to the environment. From the 8th minute until the 18th minute of the exercise, T_{sk} levels increased ($p \leq 0.05$), corresponding to heat storage inside the skin compartment of the body. On the other hand, T_{cr} responses increased significantly at all measurement points ($p \leq 0.05$) (Fig. 5), signifying consistent heat storage within the core compartment of the body.

Results of the Comparison of the ITE and IC Calculations

The difference between metabolic heat production rates calculated by ITE and IC showed a greater level of dispersion around the mean value during the first eight-minute period (CV%: 84% – 38%), as presented in Table 1. Wide-ranging correlations were observed between IC and ITE (r : 0.03–0.86), exhibiting a higher level of dispersion relative to the mean (CV%: 12 – 84%). Although the correlations between IC and ITE at the 14th and 16th minutes were substantial (r : 0.75–0.86), the differences between them were significant ($p \leq 0.05$). Metabolic heat production rates calculated by IC

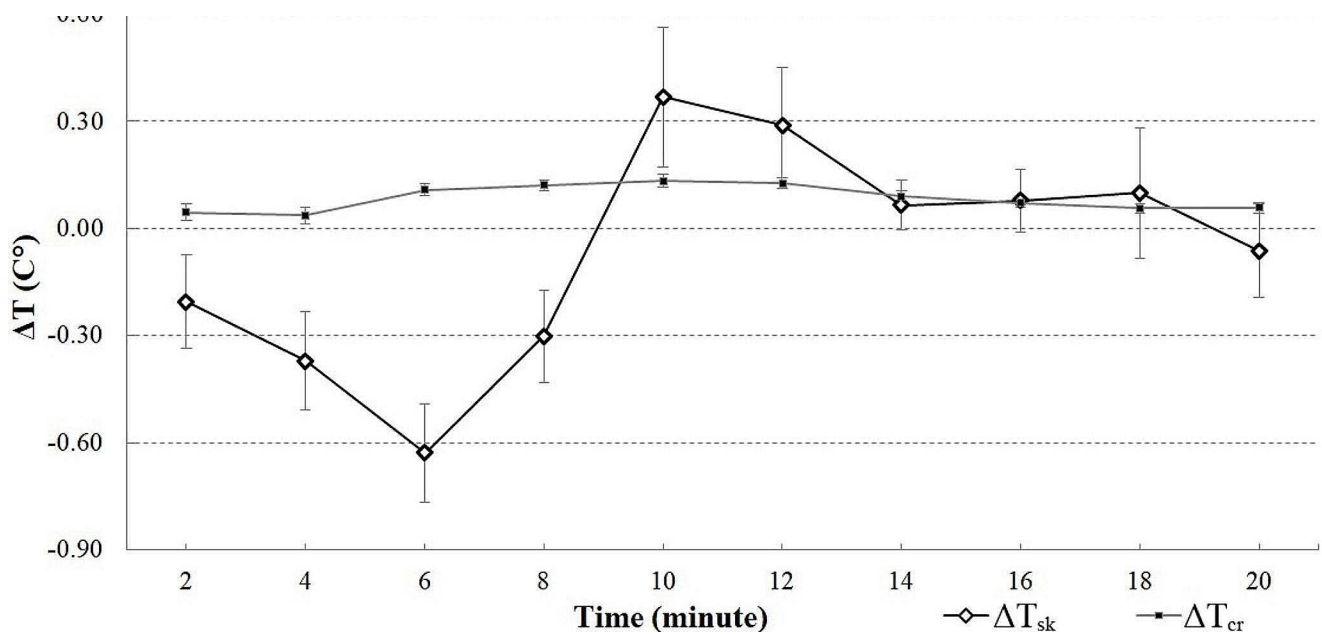


Fig. 5 Mean changes in skin and core temperatures

Table 1 Statistics for ITE and IC calculations

Duration (time, min)	IC – Heat Transfer Rate (mean ± std, W/m ²)	ITE – Heat Transfer Rate (mean ± std, W/m ²)	Bias (mean ± std, W/m ²)	t-test (p)	Effect Size	Correlation (r)	CV (%)	CV lower (%)	CV upper (%)
4	344 ± 57	87.7 ± 131	256 ± 140	0.000	1.83	0.05	74.7	48.6	101
6	351 ± 42	67.2 ± 122	284 ± 127	0.000	2.22	0.03	84.1	51.5	117
8	360 ± 49	187 ± 108	173 ± 84.0	0.000	2.06	0.66	38.4	21.6	55.3
10	357 ± 55	315 ± 136	41.9 ± 117	0.264	0.36	0.51	17.8	10.2	25.3
12	357 ± 60	315 ± 100	42.2 ± 87.2	0.140	0.48	0.50	12.0	5.66	18.4
14	360 ± 63	261 ± 92.5	100 ± 49.9	0.000	2.00	0.86	18.0	11.6	24.5
16	356 ± 60	252 ± 71.1	103 ± 47.7	0.000	2.17	0.75	18.0	12.6	23.3
18	361 ± 53	235 ± 152	125 ± 130	0.009	0.97	0.56	35.7	1.78	69.7
20	355 ± 47	232 ± 124	123 ± 100	0.002	1.23	0.64	25.6	14.4	36.8
Average	355 ± 54	217 ± 115	139 ± 98	0.046	1.48	0.51	36.0	19.8	52.3

and ITE are shown at two-minute intervals in Fig. 6, along with the results of the statistical analyses in Table 1.

Producing New Equations for Storage Rates

The mean values of the heat transfer modes during the exercise are shown in Fig. 7. It was observed that the mean heat storage rate in the skin compartment was below zero until the 8th minute. In contrast, the mean heat storage rate in the core compartment was higher than the other heat transfer modes between the 4th and 20th minute. The other heat transfer modes, except for E_{sk} , were relatively stable over $50 \text{ W}\cdot\text{m}^{-2}$. E_{sk} values increased after the 8th minute of exercise ($p \leq 0.05$). Moreover, the total energy storage rates (S) exhibit a robust correlation with the net metabolic heat production rates calculated by ITE ($r=0.984$), indicating that

heat storage rates are key determinants of the net metabolic heat production rate.

Since the heat storage rate (S) is contingent on temperature changes in the skin and core compartments (ΔT_{cr} and ΔT_{sk}), a linear regression model was established to correlate these values with S_{req} . This model provides a new calculation for the storage rates, based on data of a total of eight observation points (n) across fourteen participants (ss). The resulting linear regression model is presented in Table 2.

The new equations for the storage rates (S_{new}) were introduced in E.18. These equations were derived from the regression model that incorporates temperature changes in the skin and core compartments (ΔT_{cr} and ΔT_{sk}) over each two-minute period. According to the power analysis of the incorporation of eight observation points from fourteen participants in the linear regression model, the power ($1-\beta$) was calculated as 0.88 at a significance level (α) of 0.05. This

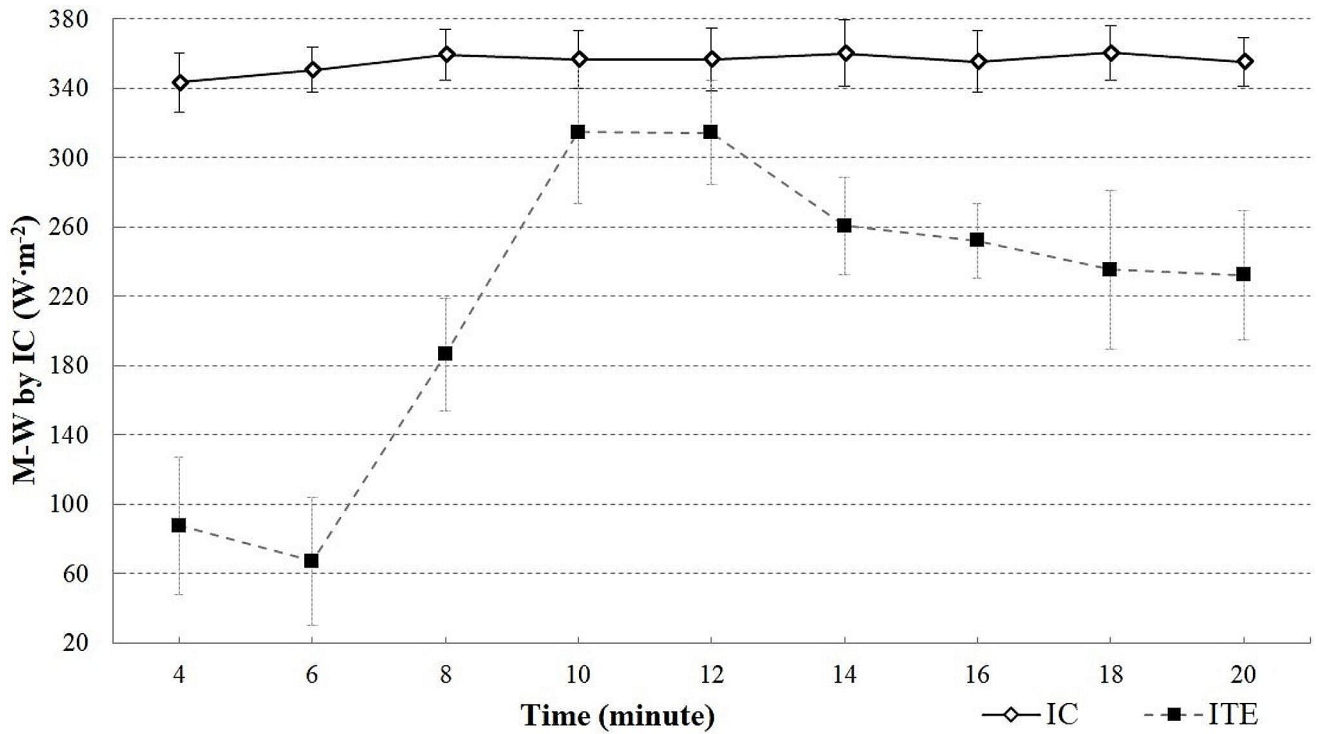


Fig. 6 Mean M-W values by IC and ITE during exercise

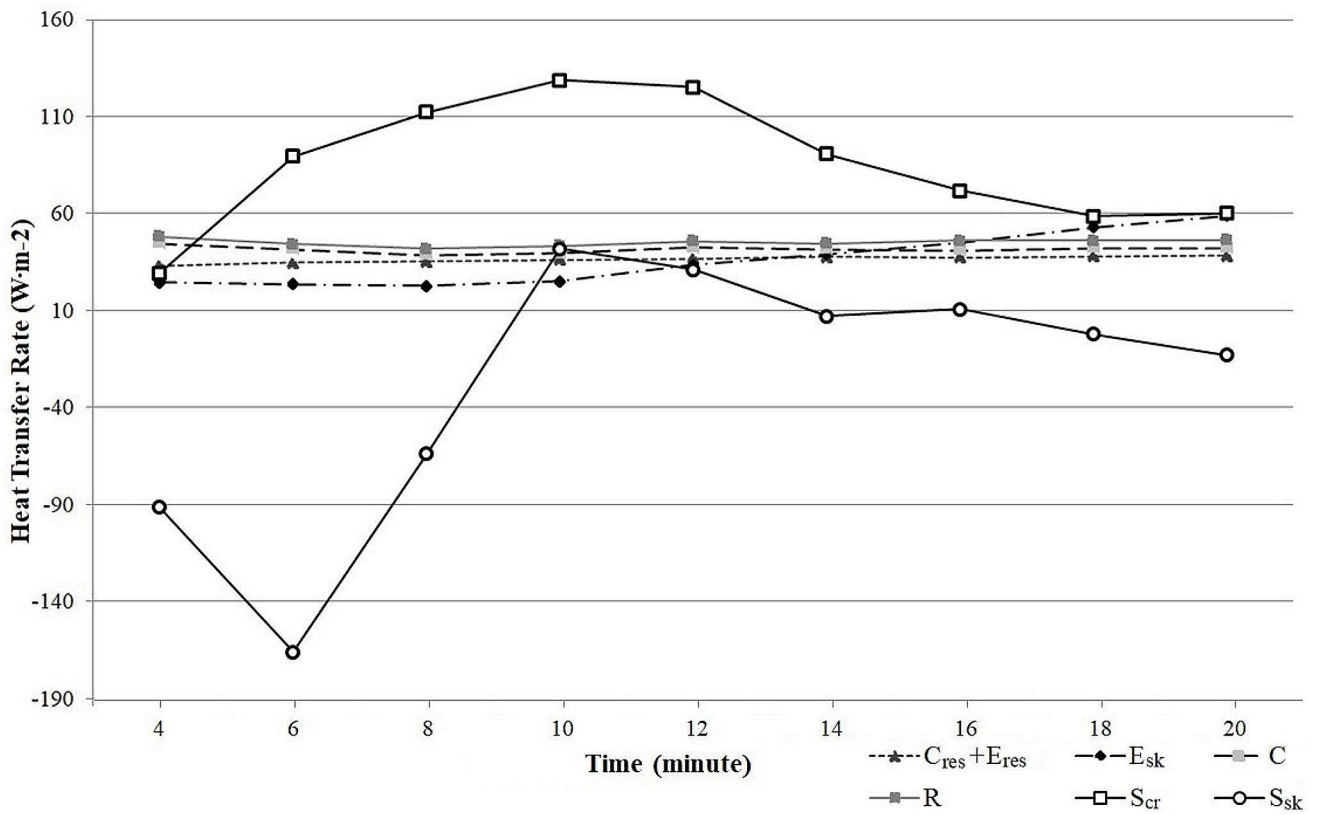


Fig. 7 Body heat transfer modes during the exercise

Table 2 Linear regression results and the new equation for the Storage Rates

	β	p-value
α	165.23	0.00
ΔT_{sk}	15.204	0.17
ΔT_{cr}	373.41	0.01
R^2	0.743	
F-statistics	8.67	0.02
Equation	$S_{new} = \alpha + \beta_1 \cdot \Delta T_{sk} + \beta_2 \cdot \Delta T_{cr} + \epsilon$	

result ensures a robust statistical foundation for the derived equation predicting heat storage rates.

$$S_{new} = 165.23 - 15.204 \times \Delta T_{sk} + 373.41 \times \Delta T_{cr} \quad [E.18]$$

Results of the Comparison of ITE_{new} and IC Calculations

After calculating the S_{new} values, ITE_{new} values were determined and compared with the IC measurements (Fig. 8). Metabolic heat production rates calculated using ITE_{new} indicated an acceptable degree of dispersion around the mean values, ranging between 3 and 6% CV%. Correlations

between ITE_{new} and IC values were consistently strong throughout the entire exercise period ($r: 0.62-0.85$) with no significant differences ($p > 0.05$). The means of ITE_{new} and IC for every two minutes of the exercise are presented in Table 3, along with the results of the statistical analyses.

Discussion

The contemporary trend toward indoor exercise spaces has highlighted the significance of understanding the dynamics of indoor thermal environments concerning human physiology (Lanza et al. 2022; Dahlan et al. 2023). This study explored the complex relationship between indoor thermal environments and human physiology during physical exercise, specifically focusing on the metabolic heat production rate. The study centered on calculating metabolic heat production rates during steady-state exercise tests in a controlled climatic chamber, incorporating human body physiological responses and indoor thermal environmental factors such as air temperature, radiant temperature, relative humidity, and air velocity.

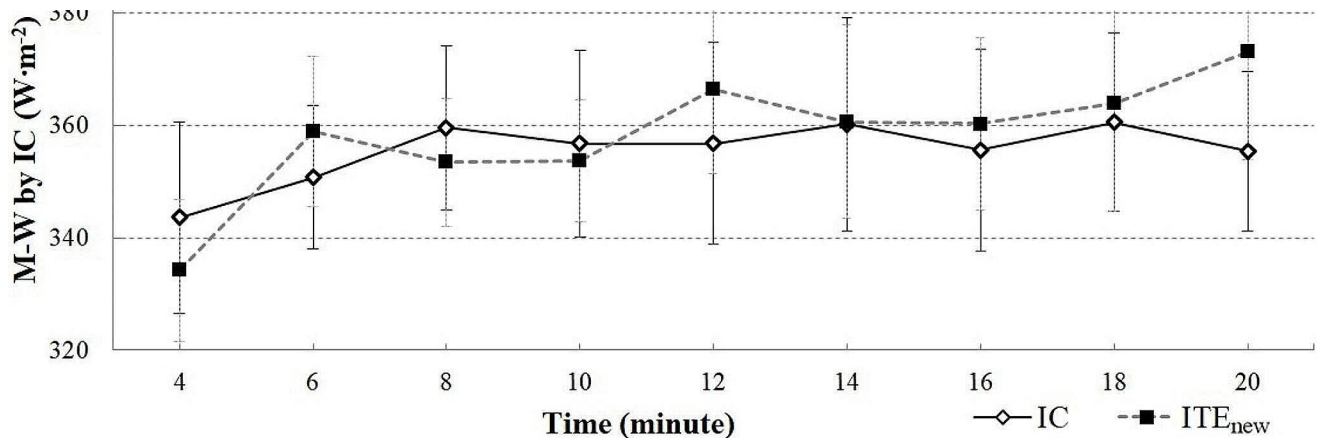


Fig. 8 Mean M-W values by IC and ITE_{new} during exercise

Table 3 Statistics for ITE_{new} and IC calculations

Duration (time, min)	IC – Heat Transfer Rate (mean ± std, W/m ²)	ITE – Heat Transfer Rate (mean ± std, W/m ²)	Bias (mean ± std, W/m ²)	t-test (p)	Effect Size	Correlation (r)	CV (%)	CV lower (%)	CV upper (%)
4	344 ± 57	334 ± 42	9.4 ± 37	0.424	0.25	0.75	4.50	2.80	6.21
6	351 ± 42	359 ± 44	-8.1 ± 37	0.482	-0.22	0.64	3.56	1.77	5.35
8	360 ± 49	353 ± 38	6.1 ± 26	0.456	0.23	0.85	2.96	1.82	4.10
10	357 ± 55	354 ± 36	3.1 ± 39	0.797	0.08	0.70	4.30	2.89	5.72
12	357 ± 60	366 ± 50	-9.7 ± 42	0.464	-0.23	0.72	4.22	5.99	5.99
14	360 ± 63	361 ± 57	-0.4 ± 36	0.969	-0.01	0.83	3.91	2.58	5.24
16	356 ± 60	360 ± 51	-4.7 ± 49	0.756	-0.10	0.62	5.13	2.68	7.58
18	361 ± 53	364 ± 64	-3.4 ± 40	0.786	-0.08	0.78	4.76	3.41	6.10
20	355 ± 47	373 ± 64	-18 ± 45	0.222	-0.39	0.70	5.63	4.08	7.18
Average	355 ± 54	358 ± 50	-2.8 ± 39	0.595	-0.05	0.73	4.33	3.11	5.94

In the study, the metabolic heat production rates were calculated using the thermal balance approach during a twenty-minute constant work rate exercise test. According to the results, the human body's thermal balance approach (ITE) did not accurately estimate the metabolic heat production rates during constant work rate exercise. This discrepancy arose due to deficiencies in the calculations of heat storage rates for the exercise condition. However, the study proposed a new equation for the body's storage rate, suggesting the possibility of accurately predicting the metabolic heat production rate during exercise.

Metabolic heat production rates by indirect calorimetry (IC) were used to determine the required evaporative heat transfer rate (E_{req}) by employing the thermal balance approach during physical exercise in the other studies (Bain et al. 2011; Vargas et al. 2019b; Ravanelli et al. 2020). Required storage rates (S_{req}) were calculated during constant work rate exercise and recovery periods by combining the thermal balance approach and indirect calorimetry (Vargas et al. 2019a). However, the present study aimed to validate the calculation of metabolic heat production rates during exercise as a replacement for indirect calorimetry.

According to the results of this study, a significant level of dispersion around the means was observed in the calculated metabolic heat production rates by ITE (CV%: 12 – 84%). Moreover, significant differences between ITE and IC were noted during the entire exercise period ($p \leq 0.05$). The results indicated that the human body's thermal balance approach did not precisely estimate the metabolic heat production rates during the exercise (r : 0.03–0.86). These differences between ITE and IC were attributed to the mode of the body's heat storage rate (S). As previously demonstrated by Kenny et al. (2008), the stored energy is the most significant among the heat modes of the exercising body, with only 53% of the stored heat from the sixty-minute exercise being removed from the body during the sixty-minute recovery. Consequently, S significantly affected the calculated ITE values, particularly until the 10th minute of the exercises. In the present study, a strong correlation was also observed between the means of ITE and S (r : 0.984).

Given that S values were associated with the temperature differences in the skin and core compartments of the body, the decrease in T_{sk} in the first eight minutes led to a greater level of dispersion around the mean estimates of IC in the present study. In the initial phase of the exercise, the decrease in T_{sk} resulted from human thermoregulation during higher metabolic activities. It has been shown that escalated cutaneous sympathetic vasoconstrictor outflow prevents skin blood flow until T_{cr} reaches approximately 37.2 °C (Kenney and Johnson 1992). Beyond this point, the vasodilatation system becomes more effective and leads the blood flow that carries excessive heat to the skin compartment (Simmons

et al. 2011). This thermoregulatory threshold corresponds to the 8th minute of the study, which is also consistent with other research findings (Torii et al. 1992; Zontak et al. 1998; Merla et al. 2010; Tanda 2018). Therefore, the metabolic heat production rate calculation until the thermoregulatory threshold needed to be approached from a different perspective to analyze thermal energy in the human body during varying exercise work rates and durations.

In order to mitigate disparities in the calculation of heat storage rate, a new equation for S was derived based on the dependence of ΔT_{cr} and ΔT_{sk} on the S_{req} for the twenty-minute exercise period. The calculated ITE_{new} values did not significantly differ from those of IC ($p > 0.05$). A strong correlation (r : 0.62–0.85) between ITE_{new} and IC was observed during the twenty-minute exercise period. Additionally, ITC data exhibited greater stability, with values consistently closer to the mean (CV%: 2.96 – 5.63%). This finding suggests that ITE_{new} values can accurately predict IC during constant work rate exercise.

The study was limited to twenty-minute steady-state exercise tests with two-minute measuring intervals. Additionally, the selection of 14 male athletes from different sports disciplines may have influenced the accuracy of the calculations. However, it is important to note that the goodness of fit for the regression model was 0.74, and the power analysis of the regression model yielded a calculated value of 0.88. The proposed ITE_{new} estimation was considered an initial step toward calculating metabolic heat production rates during exercise, emphasizing the need for a more accurate approximation of heat storage rates. The usability of the suggested equations needs validation with a larger sample size, including both female and male participants, to represent a broader population.

Conclusion

The metabolic heat production rates during exercise were calculated using the human body thermal balance approach and compared with IC measurements. The results revealed that ITE could not replace IC due to deficiencies in calculating heat storage rates, especially evident in significant deviations from the mean of T_{sk} and T_{cr} at the beginning of the exercises. A new equation to calculate the body's heat storage rate was proposed in this study to bridge this gap. Consequently, the new metabolic heat production rates calculated by ITE_{new} more accurately estimated IC values. ITE_{new} demonstrated the potential for precise metabolic heat production rate calculations during exercise. Future studies should focus on validating the obtained equation through experimental confirmation, involving larger sample sizes. Additionally, it is crucial for the equation to be substantiated

by comparisons with different studies, particularly those conducted with significantly larger sample groups. Emphasizing the need for validation through studies with more extensive and diverse participant pools will strengthen the reliability of the findings of this study.

Supplementary Information The online version contains supplementary material available at <https://doi.org/10.1007/s00484-024-02648-y>.

Acknowledgements This study was financially supported by Ege University, Scientific Research Projects Fund under grant number EGE.BAP-10.BESYO.003, and by the Scientific and Technological Research Council of Turkey (TUBITAK) Foundation under grant number 122M883.

References

- ASHRAE (2009) Chap. 9: Thermal Comfort. In: Handbook Fundamentals, pp 9.1–9.30
- Avcı AB, Balci GA, Basaran T (2024) Optimizing thermal comfort in physical exercise spaces: a study of spatial and thermal factors. *Energy Build* 303:113782. <https://doi.org/10.1016/j.enbuild.2023.113782>
- Bain AR, Deren TM, Jay O (2011) Describing individual variation in local sweating during exercise in a temperate environment. *Eur J Appl Physiol* 111:1599–1607. <https://doi.org/10.1007/s00421-010-1788-9>
- Balci GA, Basaran T, Colakoglu M (2016) Analysing visual pattern of skin temperature during submaximal and maximal exercises. *Infrared Phys Technol* 74:57–62. <https://doi.org/10.1016/j.infrared.2015.12.002>
- Çengel YA (2003) Heat transfer: a practical Approach. McGraw-Hill
- Dahlan ND, Kurmanbekova M, Yusoff WFM, Elias SM (2023) Physical activity as a Health Determinant in Tropical built environments: a multifaceted intervention. *Environ Urban ASIA* 0:1–16. <https://doi.org/10.1177/09754253221151143>
- Du Bois D, Du Bois EF (1989) A formula to estimate the approximate surface area if height and weight be known. *Nutrition* 5:303–313. <https://doi.org/10.1001/archinte.1916.00080130010002>
- Flouris AD, Schlader ZJ (2015) Human behavioral thermoregulation during exercise in the heat. *Scand J Med Sci Sports* 25:52–64. <https://doi.org/10.1111/sms.12349>
- Gagge AP, Stolwijk JAJ, Nishi Y (1972) An effective temperature scale based on a simple model of human physiological regulatory response. *Mem Fac Eng Hokkaido Univ* 13:21–36
- Gagge AP, Fobelets AP, Berglund LG (1986) A standard predictive Index of human response to thermal environment. *Am Soc Heating, Refrig Air-Conditioning Eng* 709–731
- Greenfield AM, Alba BK, Giersch GEW, Seeley AD (2023) Sex differences in thermal sensitivity and perception: implications for behavioral and autonomic thermoregulation. *Physiol Behav* 263:114126. <https://doi.org/10.1016/j.physbeh.2023.114126>
- Havenith G (2001) Individualized model of human thermoregulation for the simulation of heat stress response. *J Appl Physiol* 90:1943–1954. <https://doi.org/10.1152/jappl.2001.90.5.1943>
- Jackson AS, Pollock ML (1978) Generalized equations for predicting body density of men. *Br J Nutr* 40:497–504. <https://doi.org/10.1079/BJN19780152>
- Kang M, Kim KR, Lee J-Y, Shin J-Y (2022) Determination of thermal sensation levels for Koreans based on perceived temperature and climate chamber experiments with hot and humid settings. *Int J Biometeorol* 66:1095–1107. <https://doi.org/10.1007/s00484-022-02261-x>
- Kasprzyk T, Cholewka A, Kuciewicz M et al (2019) A quantitative thermal analysis of cyclists' thermo-active base layers. *J Therm Anal Calorim* 136:1689–1699. <https://doi.org/10.1007/s10973-018-7775-9>
- Kenney WL, Johnson JM (1992) Control of skin blood flow during exercise. *Med Sci Sports Exerc* 24:303–312
- Kenny GP, Webb P, Ducharme MB et al (2008) Calorimetric measurement of postexercise net heat loss and residual body heat storage. *Med Sci Sports Exerc* 40:1629–1636. <https://doi.org/10.1249/MSS.0b013e31817751cb>
- Lanza K, Gohlke J, Wang S et al (2022) Climate change and physical activity: ambient temperature and urban trail use in Texas. *Int J Biometeorol* 66:1575–1588. <https://doi.org/10.1007/s00484-022-02302-5>
- Lin Y, Jin H, Jin Y, Kang J (2023) Experimental study on the effects of exercise intensity and thermal environment on thermal responses. *Build Environ* 232:110067. <https://doi.org/10.1016/j.buildenv.2023.110067>
- Marins JCB, Moreira DG, Cano SP et al (2014) Time required to stabilize thermographic images at rest. *Infrared Phys Technol* 65:30–35. <https://doi.org/10.1016/j.infrared.2014.02.008>
- Merla A, Mattei PA, Di Donato L, Romani GL (2010) Thermal imaging of cutaneous temperature modifications in runners during graded Exercise. *Ann Biomed Eng* 38:158–163. <https://doi.org/10.1007/s10439-009-9809-8>
- Nishi Y (1981) Chap. 2 measurement of Thermal Balance of Man. In: Cena K, Clark JA (eds) *Studies in environmental science*. Elsevier, pp 29–39
- Parsons K (2014) *Human Thermal Environments, The Effects of Hot, Moderate, and Cold Environments on Human Health, Comfort, and Performance*, Third Edition. CRC Press, Boca Raton
- Qi L, Wu Q, Zhang L, Liu J (2022) Effect of environmental parameters on heat transfer characteristics and thermal sensation of human body with step change of temperature. *Heat Mass Transf* 58:873–885. <https://doi.org/10.1007/s00231-021-03151-5>
- Qingqing W, Jianhua L (2020) Comparative study on differences of human thermal characteristics in cabin between driving and idle state. *Heat Mass Transf* 56:2255–2264. <https://doi.org/10.1007/s00231-020-02850-9>
- Ravanelli N, Imbeault P, Jay O (2020) Steady-state sweating during exercise is determined by the evaporative requirement for heat balance independently of absolute core and skin temperatures. *J Physiol* 598:2607–2619. <https://doi.org/10.1113/JP279447>
- Schneider DA, Phillips SE, Stoffolano S (1993) The simplified V-slope method of detecting the gas exchange threshold. *Med Sci Sport Exerc*. <https://doi.org/10.1249/00005768-199310000-00015>. 25:1180??1184
- Simmons GH, Wong BJ, Holowatz LA, Kenney WL (2011) Changes in the control of skin blood flow with exercise training: where do cutaneous vascular adaptations fit in? *Exp Physiol* 96:822–828. <https://doi.org/10.1113/expphysiol.2010.056176>
- Takada S, Kobayashi H, Matsushita T (2009) Thermal model of human body fitted with individual characteristics of body temperature regulation. *Build Environ* 44:463–470. <https://doi.org/10.1016/j.buildenv.2008.04.007>
- Tanabe S, Suzuki T, Kimura K, Horikawa S (1995) Numerical Simulation Model of Thermal Regulation of Man with 16 Body Parts of Evaluating Thermal Environment (Part 1 Heat Transfer at Skin Surface and Comparison with SET* and Stolwijk Model). In: *Summaries of Technical Papers of Annual Meeting, Architectural Institute of Japan*
- Tanda G (2018) Total body skin temperature of runners during treadmill exercise. *J Therm Anal Calorim* 131:1967–1977. <https://doi.org/10.1007/s10973-017-6634-4>

- Torii M, Yamasaki M, Sasaki T, Nakayama H (1992) Fall in skin temperature of exercising man. *Br J Sports Med* 26:29–32. <https://doi.org/10.1136/bjsm.26.1.29>
- Vargas NT, Chapman CL, Johnson BD et al (2019a) Thermal behavior augments heat loss following low intensity Exercise. *Int J Environ Res Public Health* 17:20. <https://doi.org/10.3390/ijerph17010020>
- Vargas NT, Chapman CL, Johnson BD et al (2019b) Exercise intensity independently modulates thermal behavior during exercise recovery but not during exercise. *J Appl Physiol* 126:1150–1159. <https://doi.org/10.1152/jappphysiol.00992.2018>
- Wasserfurth P, Palmowski J, Hahn A, Krüger K (2020) Reasons for and Consequences of Low Energy Availability in female and male athletes: Social Environment, adaptations, and Prevention. *Sport Med - Open* 6:44. <https://doi.org/10.1186/s40798-020-00275-6>
- Whipp BJ, Ward SA, Lamarra N et al (1982) Parameters of ventilatory and gas exchange dynamics during exercise. *J Appl Physiol* 52:1506–1513. <https://doi.org/10.1152/jappl.1982.52.6.1506>
- Zontak A, Sideman S, Verbitsky O, Beyar R (1998) Dynamic thermography: analysis of hand temperature during exercise. *Ann Biomed Eng* 26:988–993. <https://doi.org/10.1114/1.33>
- Zora S, Balci G, Colakoglu M, Basaran T (2017) Associations between Thermal and physiological responses of human body during Exercise. *Sports* 5:97. <https://doi.org/10.3390/sports5040097>

Publisher's Note Springer Nature remains neutral with regard to jurisdictional claims in published maps and institutional affiliations.

Springer Nature or its licensor (e.g. a society or other partner) holds exclusive rights to this article under a publishing agreement with the author(s) or other rightsholder(s); author self-archiving of the accepted manuscript version of this article is solely governed by the terms of such publishing agreement and applicable law.